

November 8, 2018

## DARK MATTER IN SUSY MODELS

R. ARNOWITT, B. DUTTA AND Y. SANTOSO

*Center For Theoretical Physics, Department of Physics,  
Texas A&M University, College Station TX 77843-4242*

Direct detection experiments for neutralino dark matter in the Milky Way are examined within the framework of SUGRA models with R-parity invariance and grand unification at the GUT scale,  $M_G$ . Models of this type apply to a large number of phenomena, and all existing bounds on the SUSY parameter space due to current experimental constraints are included. For models with universal soft breaking at  $M_G$  (mSUGRA), the Higgs mass and  $b \rightarrow s\gamma$  constraints imply that the gaugino mass,  $m_{1/2}$ , obeys  $m_{1/2} > (300\text{--}400)\text{GeV}$  putting most of the parameter space in the co-annihilation domain where there is a relatively narrow band in the  $m_0 - m_{1/2}$  plane. For  $\mu > 0$  we find that the neutralino -proton cross section  $\gtrsim 10^{-10}$  pb for  $m_{1/2} < 1$  TeV, making almost all of this parameter space accessible to future planned detectors. For  $\mu < 0$ , however, there will be large regions of parameter space with cross sections  $< 10^{-12}$  pb, and hence inaccessible experimentally. If, however, the muon magnetic moment anomaly is confirmed, then  $\mu > 0$  and  $m_{1/2} \lesssim 800$  GeV. Models with non-universal soft breaking in the third generation and Higgs sector can allow for new effects arising from additional early universe annihilation through the  $Z$ -channel pole. Here cross sections that will be accessible in the near future to the next generation of detectors can arise, and can even rise to the large values implied by the DAMA data. Thus dark matter detectors have the possibility of studying the the post-GUT physics that control the patterns of soft breaking.

PRESENTED AT

NON-ACCELERATOR NEW PHYSICS

Dubna, Russia,  
June 19–23, 2001

# 1 Introduction

The recent BOOMERanG, Maxima and DASI data has allowed a relatively precise determination of the mean amount of dark matter in the universe, and these results are consistent with other astronomical observations. Within the Milky Way itself, the amount of dark matter is estimated to be

$$\rho_{DM} \cong (0.3 - 0.5) \text{GeV}/\text{cm}^3 \quad (1)$$

Supersymmetry with R-parity invariance possesses a natural candidate for cold dark matter (CDM), the lightest neutralino,  $\tilde{\chi}_1^0$ , and SUGRA models predict a relic density consistent with the astronomical observations of dark matter. Several methods for detecting the Milky Way neutralinos exist:

(1) Annihilation of  $\tilde{\chi}_1^0$  in the halo of the Galaxy leading to anti-proton or positron signals. There have been several interesting analyses of these possibilities [1, 2], but there are still uncertainties as to astronomical backgrounds.

(2) Annihilation of the  $\tilde{\chi}_1^0$  in the center of the Sun or Earth leading to neutrinos and detection of the energetic  $\nu_\mu$  by neutrino telescopes (AMANDA, Ice Cube, ANTARES). Recent analyses [3, 4] indicate that these detectors can be sensitive to such signals, but for the Minimal Supersymmetric Standard Model (MSSM) one requires  $m_{\tilde{\chi}_1^0} > 200$  GeV (i.e.  $m_{1/2} > 500$  GeV) and  $\tan \beta > 10$ , and for SUGRA models one is restricted to  $\tan \beta > 35$  [3].

(3) Direct detection by scattering of incident  $\tilde{\chi}_1^0$  on nuclear targets of terrestrial detectors. Current detectors are sensitive to such events for  $\tilde{\chi}_1^0 - p$  cross sections in the range

$$\sigma_{\tilde{\chi}_1^0 - p} \gtrsim 1 \times 10^{-6} \text{pb} \quad (2)$$

with a possible improvement by a factor of 10 - 100 in the near future. Future detectors (GENIUS, Cryoarray, ZEPLIN IV) may be sensitive down to  $(10^{-9} - 10^{-10})$  pb and we will see that this would be sufficient to cover the parameter space of most SUGRA models.

In the following we will consider SUGRA models with R-parity invariance based on grand unification at the GUT scale  $M_G \cong 2 \times 10^{16}$  GeV. In particular, we will consider two classes of models: Minimal supergravity models (mSUGRA [5, 6]) with universal soft breaking masses at  $M_G$ , and non-universal models with non universal soft breaking at  $M_G$  for the Higgs bosons and the third generation of squarks and sleptons. Here the gaugino masses ( $m_{1/2}$ ) and the cubic soft breaking masses ( $A_0$ ) at  $M_G$  are assumed universal.

SUGRA models apply to a wide range of phenomena, and data from different experiments interact with each other to greatly sharpen the predictions. We list here the important experimental constraints:

Higgs mass:  $m_h > 114$  GeV [7]. The theoretical calculation of  $m_h$  still has an error of  $\sim 3$  GeV, and so we will (conservatively) interpret this bound to mean  $m_h(\text{theory}) > 111$  GeV.

$b \rightarrow s\gamma$  branching ratio. We take a  $2\sigma$  range around the central CLEO value [8]:

$$1.8 \times 10^{-4} \leq B(B \rightarrow X_s \gamma) \leq 4.5 \times 10^{-4} \quad (3)$$

$\tilde{\chi}_1^0$  relic density: We assume here

$$0.02 \leq \Omega_{\text{DM}} h^2 \leq 0.25 \quad (4)$$

The lower bound takes into account of the possibility that there is more than one species of DM. However, results are insensitive to raising it to 0.05 or 0.10.

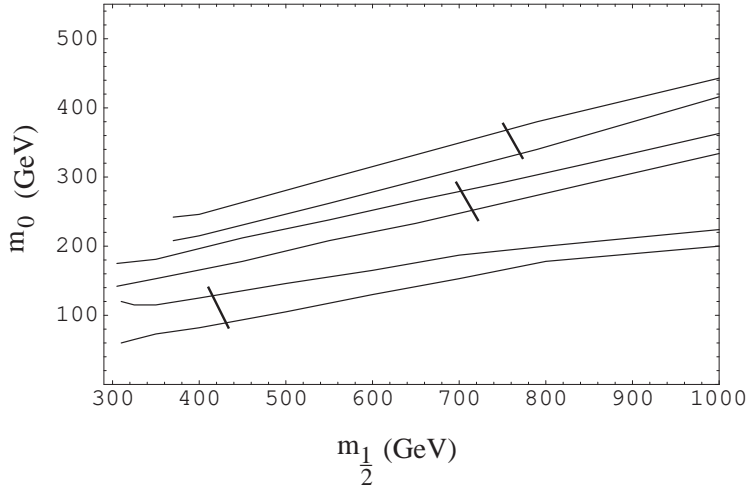


Figure 1: Corridors in the  $m_0 - m_{1/2}$  plane allowed by the relic density constraints for (bottom to top)  $\tan \beta = 10, 30, 40$ ,  $A_0 = 0$  and  $\mu > 0$ . The lower bound on  $m_{1/2}$  is due to the  $m_h$  lower bound for  $\tan \beta = 10$ , due to the  $b \rightarrow s\gamma$  bound for  $\tan \beta = 40$ , while both these contribute equally for  $\tan \beta = 30$ . The short lines cutting the channels represent upper bound from the  $g_\mu - 2$  experiment. [17]

Muon  $a_\mu = (g_\mu - 2)/2$  anomaly. The Brookhaven E821 experiment [9] reported a  $2.6\sigma$  deviation from the Standard Model value in their measurement of the muon magnetic moment. Recently a sign error in the theoretical calculation [10, 11] has reduced this to a  $1.6\sigma$  anomaly, though recent measurements [12] used to calculate the hadronic contribution may have raised the deviation. Since there is a great deal of more data currently being analyzed (with results due this spring) that will reduce the errors by a factor of  $\sim 2.5$ , we will assume here that there is a deviation in  $a_\mu$  due to SUGRA of amount

$$11 \times 10^{-10} \leq a_\mu^{\text{SUGRA}} \leq 75 \times 10^{-10} \quad (5)$$

We will, however, state our results with and without including this anomaly.

To illustrate how the different experimental constraints affect the SUSY parameter space, we consider the mSUGRA example:

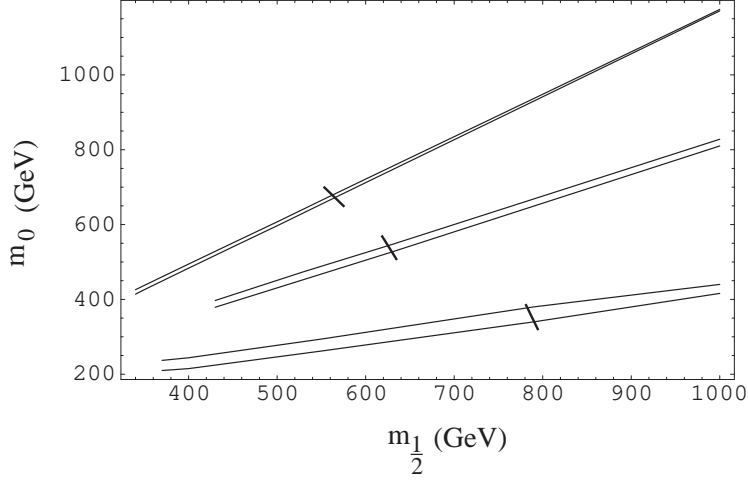


Figure 2: Corridors in the  $m_0 - m_{1/2}$  plane allowed by the relic density constraint for  $\tan\beta = 40$ ,  $\mu > 0$  and (bottom to top)  $A_0 = 0, -2m_{1/2}, 4m_{1/2}$ . the curves terminate at the lower end due to the  $b \rightarrow s\gamma$  constraint except for  $A_0 = 4m_{1/2}$  which terminates due to the  $m_h$  constraint. The short lines cutting the corridors represent the upper bound on  $m_{1/2}$  due to the  $g_\mu - 2$  experiment. [17]

(1) The  $m_h$  and  $b \rightarrow s\gamma$  constraints put a lower bound on  $m_{1/2}$ :

$$m_{1/2} \gtrsim (300 - 400)\text{GeV} \quad (6)$$

which means  $m_{\tilde{\chi}_1^0} \gtrsim (120 - 160)\text{GeV}$  (since  $m_{\tilde{\chi}_1^0} \cong 0.4m_{1/2}$ ). (2) Eq.(6) now means that most of the parameter space is in the  $\tilde{\tau}_1 - \tilde{\chi}_1^0$  co-annihilation domain in the relic density calculation. Then  $m_0$  (the squark and slepton soft breaking mass) is approximately determined by  $m_{1/2}$  as can be seen in Figs. 1 and 2. (3) If we include the  $a_\mu$  anomaly, since  $a_\mu^{\text{SUGRA}}$  is a decreasing function of  $m_{1/2}$  and  $m_0$ , the lower bound of Eq.(5) produces an upper bound on  $m_{1/2}$  and the positive sign of  $a_\mu$  implies that the  $\mu$  parameter is positive. In addition one gets a lower bound on  $\tan\beta$  of  $\tan\beta > 5$ . Thus the parameter space has begun to be strongly constrained, allowing for more precise predictions. In order to carry out detailed calculations, however, it is necessary to include a number of analyses to obtain accurate results. We list some of these here:

Two loop gauge and one loop Yukawa renormalization group equations (RGE) are used in going from  $M_G$  to the electroweak scale  $M_{\text{EW}}$ , and QCD RGE are used below  $M_{\text{EW}}$  for the light quark contributions. Two loop and pole mass corrections are included in the calculation of  $m_h$ . One loop corrections to  $m_b$  and  $m_\tau$  [13, 14] are included which are important at large  $\tan\beta$ . Large  $\tan\beta$  NLO SUSY corrections to  $b \rightarrow s\gamma$  [15, 16] are included. In calculating the relic density, all stau-neutralino co-annihilation channels are included, and this calculation is done in a fashion valid for both small and large  $\tan\beta$ .

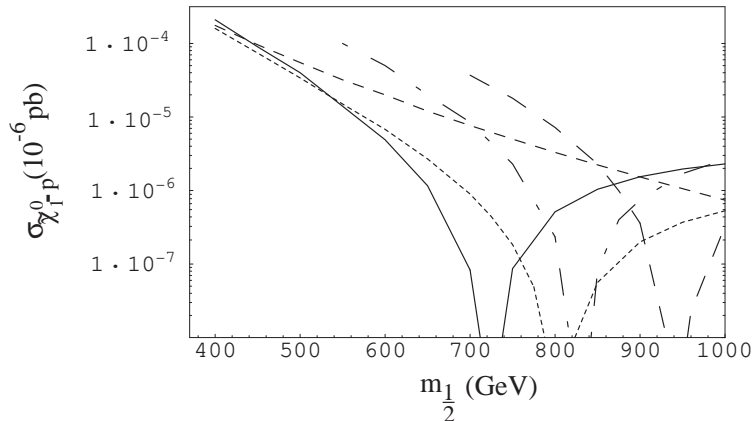


Figure 3:  $\sigma_{\tilde{\chi}_1^0-p}$  for mSUGRA for  $\mu < 0$ ,  $A_0 = 1500$  GeV, for  $\tan\beta = 6$  (short dash),  $\tan\beta = 8$  (dotted),  $\tan\beta = 10$  (solid),  $\tan\beta = 20$  (dot-dash),  $\tan\beta = 25$  (dashed). Note that the  $\tan\beta = 6$  curve terminates at low  $m_{1/2}$  due to the Higgs mass constraint, and the other curves terminate at low  $m_{1/2}$  due to the  $b \rightarrow s\gamma$  constraint [18].

We do not include Yukawa unification or proton decay constraints, since these depend sensitively on post-GUT physics, about which little is known.

## 2 mSUGRA MODEL

The mSUGRA model is the simplest, and hence most predictive of the supergravity models in that it depends on only four new parameters and one sign (in addition to the usual SM parameters). We take these new parameters to be  $m_0$  and  $m_{1/2}$  (the universal soft breaking scalar and gaugino masses at  $M_G$ ),  $A_0$  (the universal cubic soft breaking mass at  $M_G$ ),  $\tan\beta = \langle H_2 \rangle / \langle H_1 \rangle$  at the electroweak scale (where  $\langle H_2 \rangle$  gives rise to up quark masses and  $\langle H_1 \rangle$  to down quark masses) and the sign of  $\mu$  (the Higgs mixing parameter which appears in the superpotential as  $\mu H_1 H_2$ ). We examine these parameters over the range  $m_0, m_{1/2} \leq 1$  TeV,  $2 < \tan\beta < 50$ ,  $|A_0| \leq 4m_{1/2}$ . The bound on  $m_{1/2}$  corresponds to the gluino mass bound of  $m_{\tilde{g}} < 2.5$  GeV which is also the reach of the LHC.

The relic density analysis involves calculating the annihilation cross section for neutralinos in the early universe. This characteristically proceeds through  $Z$  and Higgs  $s$ -channel poles ( $Z, h, H, A$  where  $H$  and  $A$  are heavy CP even and CP odd Higgs bosons) and through  $t$ -channel sfermion poles. However, if there is a second particle which becomes nearly degenerate with the neutralino, one must include it in the early universe annihilation processes, which then leads to the co-annihilation phenomena. In mSUGRA models, this accidental near degeneracy occurs naturally for the light stau,  $\tilde{\tau}_1$ . One can understand this semi-quantitatively by considering the low and intermediate  $\tan\beta$  region

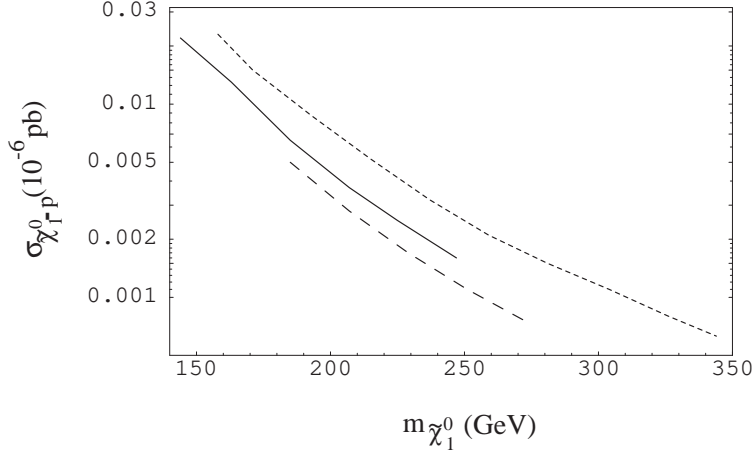


Figure 4:  $\sigma_{\tilde{\chi}_1^0-p}$  as a function of the neutralino mass  $m_{\tilde{\chi}_1^0}$  for  $\tan\beta = 40$ ,  $\mu > 0$  for  $A_0 = -2m_{1/2}, 4m_{1/2}, 0$  from bottom to top. The curves terminate at small  $m_{\tilde{\chi}_1^0}$  due to the  $b \rightarrow s\gamma$  constraint for  $A_0 = 0$  and  $-2m_{1/2}$  and due to the Higgs mass bound ( $m_h > 114$  GeV) for  $A_0 = 4m_{1/2}$ . The curves terminate at large  $m_{\tilde{\chi}_1^0}$  due to the lower bound on  $a_\mu$  of Eq. (5)[17].

where the RGE give for the right selectron,  $\tilde{e}_R$ , and the neutralino the following masses at the electroweak scale:

$$m_{\tilde{e}_R}^2 = m_0^2 + 0.15m_{1/2}^2 - \sin^2\theta_W M_W^2 \cos 2\beta \quad (7)$$

$$m_{\tilde{\chi}_1^0}^2 = 0.16m_{1/2}^2 \quad (8)$$

the numerics coming from the RGE analysis. The last term in Eq. (7)  $\cong (40 \text{ GeV})^2$ . Thus for  $m_0 = 0$  the  $\tilde{e}_R$  will become degenerate with the  $\tilde{\chi}_1^0$  at  $m_{1/2} \cong 400$  GeV, and co-annihilation thus begins at  $m_{1/2} \cong (350 - 400)$  GeV. As  $m_{1/2}$  increases,  $m_0$  must be raised in lock step (to keep  $m_{\tilde{e}_R} > m_{\tilde{\chi}_1^0}$ ). More precisely, it is the light stau, which is the lightest slepton that dominates the co-annihilation phenomena. However, one ends up with corridors in the  $m_0 - m_{1/2}$  plane for allowed relic density with  $m_0$  closely correlated with  $m_{1/2}$  increasing as  $m_{1/2}$  does, as seen in Figs. 1 and 2.

For dark matter detectors with heavy nuclei targets, the spin independent neutralino - nucleus cross section dominates, which allows one to extract the  $\tilde{\chi}_1^0$ -proton cross section,  $\sigma_{\tilde{\chi}_1^0-p}$ . The basic quark diagrams for this scattering go through s-channel squark poles and t-channel Higgs (h, H) poles. The general features of  $\sigma_{\tilde{\chi}_1^0-p}$  that explain its properties are the following:

$$\sigma_{\tilde{\chi}_1^0-p} \text{ increases with increasing } \tan\beta \quad (9)$$

$$\sigma_{\tilde{\chi}_1^0-p} \text{ decreases with increasing } m_{1/2} \text{ and increasing } m_0 \quad (10)$$

Since co-annihilation generally correlates  $m_0$  and  $m_{1/2}$ , if  $m_{1/2}$  increases so does  $m_0$  (at fixed  $\tan\beta$  and  $A_0$ ).

The smallest cross sections occur for the case  $\mu < 0$ . This is because a special cancellation can occur over a fairly wide range of  $\tan\beta$  and  $m_{1/2}$  [19, 18] driving the cross section below  $10^{-13}$  pb. This is illustrated in Fig. 3. In these regions, there would be no hope for currently planned dark matter detectors to be able to detect Milky Way neutralinos. However, if the  $a_\mu$  anomaly is confirmed by the new BNL E821 data (currently being analyzed), then  $\mu < 0$  is forbidden, and the special cancelations do not occur for  $\mu > 0$ . Large cross sections can then occur for large tanbeta. Thus is seen in Fig. 4 for  $\tan\beta = 40$ , with  $m_h > 114$  GeV. If the Higgs mass bound were to rise, the lower bounds on  $m_{1/2}$  would increase. Thus for  $m_h > 120$  GeV, one has  $m_{\tilde{\chi}_1^0} > (200, 215, 246)$  GeV for  $A_0 = (-2, 0, 4)m_{1/2}$ .

The lowest cross sections for  $\mu > 0$  are expected to occur for small tanbeta and large  $m_{1/2}$ . This is seen in Fig. 5 for  $\tan\beta = 10$  where one also sees that decreasing  $A_0$  gives smaller cross sections. In general one finds

$$\sigma_{\tilde{\chi}_1^0-p} \gtrsim 10^{-10} \text{ pb for } \mu > 0, m_{1/2} < 1 \text{ TeV} \quad (11)$$

Such cross sections are within the reach of future planned detectors.

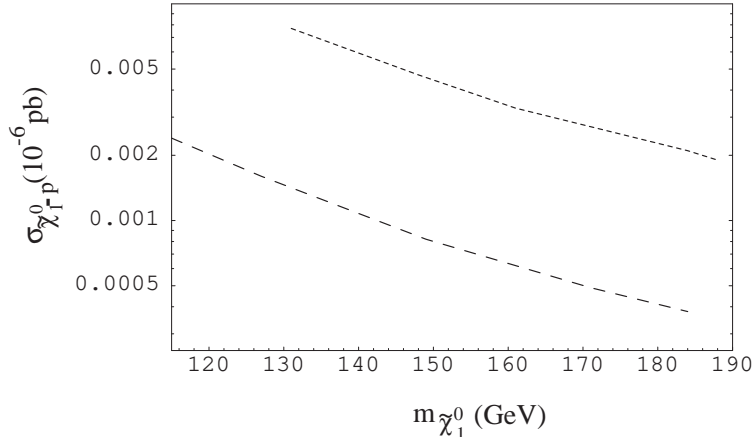


Figure 5:  $\sigma_{\tilde{\chi}_1^0-p}$  as a function of  $m_{\tilde{\chi}_1^0}$  for  $\tan\beta = 10$ ,  $\mu > 0$ ,  $m_h > 114$  GeV for  $A_0 = 0$  (upper curve),  $A_0 = -4m_{1/2}$  (lower curve). The termination at low  $m_{\tilde{\chi}_1^0}$  is due to the  $m_h$  bound for  $A_0 = 0$ , and the  $b \rightarrow s\gamma$  bound for  $A_0 = -4m_{1/2}$ . The termination at high  $m_{\tilde{\chi}_1^0}$  is due to the lower bound on  $a_\mu$  of Eq. (5)[17].

### 3 NON-UNIVERSAL MODELS

New results can occur if we relax the universality of the squark, slepton and soft breaking Higgs masses at  $M_G$ . To maintain the flavor changing neutral current bounds, we do this

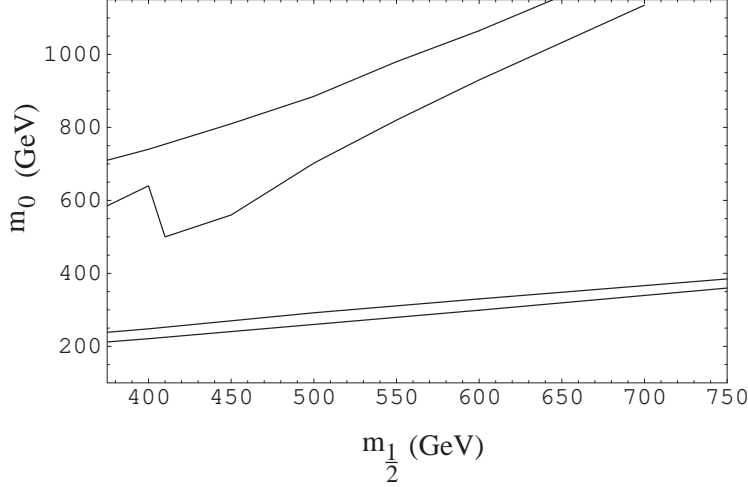


Figure 6: Effect of a nonuniversal Higgs soft breaking mass enhancing the  $Z^0$  s-channel pole contribution in the early universe annihilation, for the case of  $\delta_2 = 1$ ,  $\tan \beta = 40$ ,  $A_0 = m_{1/2}$ ,  $\mu > 0$ . The lower band is the usual  $\tilde{\tau}_1$  coannihilation region. The upper band is an additional region satisfying the relic density constraint arising from increased annihilation via the  $Z^0$  pole due to the decrease in  $\mu^2$  increasing the higgsino content of the neutralino[18].

only in the third generation and for the Higgs bosons. One may parameterize the soft breaking masses at  $M_G$  as follows:

$$\begin{aligned}
m_{H_1}^2 &= m_0^2(1 + \delta_1); & m_{H_2}^2 &= m_0^2(1 + \delta_2); \\
m_{q_L}^2 &= m_0^2(1 + \delta_3); & m_{t_R}^2 &= m_0^2(1 + \delta_4); & m_{\tau_R}^2 &= m_0^2(1 + \delta_5); \\
m_{b_R}^2 &= m_0^2(1 + \delta_6); & m_{l_L}^2 &= m_0^2(1 + \delta_7).
\end{aligned} \tag{12}$$

with  $-1 \leq \delta_i \leq +1$ . While the non-universal models introduce a number of new parameters, it is possible to understand qualitatively what effects they produce on dark matter detection rates, since the parameter  $\mu^2$  governs much of the physics. Thus as  $\mu^2$  decreases (increases), the higgsino content of the neutralino increases (decreases), and then  $\sigma_{\tilde{\chi}_1^0-p}$  increases (decreases). One can further see semi-quantitatively the dependence of  $\mu^2$  on the non-universal parameters for low and intermediate  $\tan \beta$  where the RGE may be solved analytically [20]:

$$\begin{aligned}
\mu^2 &= \frac{t^2}{t^2 - 1} \left[ \left( \frac{1 - 3D_0}{2} + \frac{1}{t^2} \right) + \frac{1 - D_0}{2} (\delta_3 + \delta_4) \right. \\
&\quad \left. - \frac{1 + D_0}{2} \delta_2 + \frac{\delta_1}{t^2} \right] m_0^2 + \text{universal parts} + \text{loop corrections}.
\end{aligned} \tag{13}$$

where  $t = \tan \beta$  and  $D_0 \cong 1 - (m_t/200 \sin \beta)^2$ . In general  $D_0$  is small i.e.  $D_0 \cong 0.25$ , and one sees that the universal part of the  $m_0^2$  contribution is quite small, and it does not take



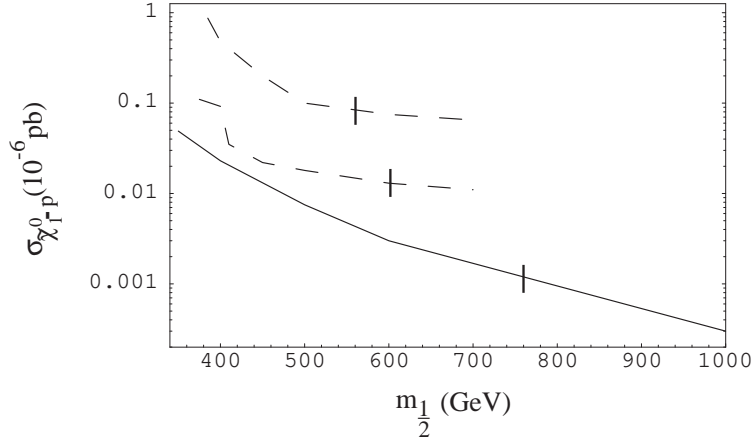


Figure 7:  $\sigma_{\tilde{\chi}_1^0-p}$  as a function of  $m_{1/2}$  ( $m_{\tilde{\chi}_1^0} \approx 0.4m_{1/2}$ ) for  $\tan\beta = 40$ ,  $\mu > 0$ ,  $m_h > 114$  GeV,  $A_0 = m_{1/2}$  for  $\delta_2 = 1$ . The lower curve is for the  $\tilde{\tau}_1 - \tilde{\chi}_1^0$  co-annihilation channel, and the dashed band is for the  $Z$  s-channel annihilation allowed by non-universal soft breaking. The curves terminate at low  $m_{1/2}$  due to the  $b \rightarrow s\gamma$  constraint. The vertical lines show the termination at high  $m_{1/2}$  due to the lower bound on  $a_\mu$  of Eq. (5)[21].

a great deal of non-universal contribution to produce additional effects.

Most interesting things happen when  $\mu^2$  is decreased, since the increased Higgsino content of the neutralino increases the  $\tilde{\chi}_1^0 - \tilde{\chi}_1^0 - Z$  coupling, and this coupling opens a new annihilation channel through the  $Z$ -pole in the relic density calculations. As a simple example we consider the case where only the  $H_2$  soft breaking mass is affected i. e.  $\delta_2 = 1$  and all other  $\delta_i = 0$ . Fig. 6 shows the new allowed region in the  $m_0 - m_{1/2}$  plane for  $\tan\beta = 40$ ,  $A_0 = m_{1/2}$ ,  $\mu > 0$ , and Fig. 7 shows the corresponding effect on the neutralino - proton cross section. One sees that the co-annihilation corridor is significantly raised and widened due to the new  $Z$ -channel annihilation, and the cross section is significantly increased. The next round of upgraded dark matter detectors should be able to reach parts of this parameter space if such a non-universality were to occur.

As a second example we consider a soft breaking pattern consistent with an  $SU(5)$  invariant model with  $\delta_{10}(=\delta_3=\delta_4=\delta_5)=-0.7$ , and all other  $\delta_i=0$ . Here the  $\tilde{\tau}_R$  soft breaking mass is reduced, i.e.  $m_{\tilde{\tau}_R}^2 = m_0^2(1+\delta_5) < m_0^2$ . Thus the  $\tilde{\tau}_1 - \tilde{\chi}_1^0$  co-annihilation occurs at a larger value of  $m_0$  than in mSUGRA. In addition again a new  $Z$ -channel neutralino annihilation channel occurs since  $\mu^2$  is reduced. The effects are shown in Figs. 8 and 9 for  $\tan\beta = 40$ ,  $A_0 = m_{1/2}$ ,  $\mu > 0$ . Again the cross sections are larger, and should be accessible to CDMS when it moves to the Soudan mine and to GENIUS.

The maximum value of  $\sigma_{\tilde{\chi}_1^0-p}$  for fixed  $\tan\beta$  and  $A_0$  occurs when we chose the non-universality to minimize  $\mu^2$ . This occurs when  $\delta_{1,3,4} < 0$  and  $\delta_2 > 0$ . This is shown in Fig. 10 where the maximum cross section is plotted for  $A_0 = 0$ ,  $\tan\beta = 12$  (upper curve),  $\tan\beta = 7$  (lower curve). The bound that  $m_h > 114$  GeV, eliminates the region

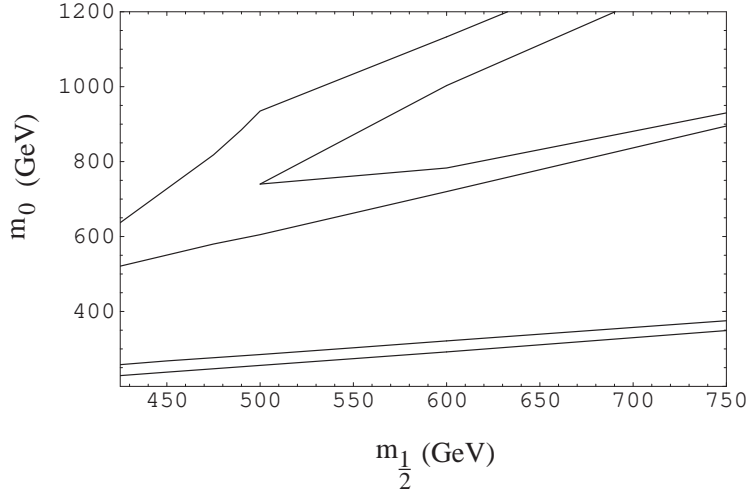


Figure 8: Allowed regions in the  $m_0 - m_{1/2}$  plane for the case  $\tan\beta = 40$ ,  $A_0 = m_{1/2}$ ,  $\mu > 0$ . The bottom curve is the mSUGRA  $\tilde{\tau}_1$  coannihilation band of Fig. 1 (shown for reference). The middle band is the actual  $\tilde{\tau}_1$  coannihilation band when  $\delta_{10} = -0.7$ . The top band is an additional allowed region due to the enhancement of the  $Z^0$  s-channel annihilation arising from the nonuniversality lowering the value of  $\mu^2$  and hence raising the higgsino content of the neutralino. For  $m_{1/2} \gtrsim 500$  GeV, the two bands overlap [18].

with  $m_{\tilde{\chi}_1^0} < 100$  GeV. However, one sees for this case that it is possible to have detection cross sections in the region of the DAMA data.

## 4 CONCLUSIONS

We have discussed here direct detection of Milky Way neutralinos for SUGRA type models with R-parity invariance and grand unification at the GUT scale. By combining data from a variety of sources, e.g. Higgs mass bound,  $b \rightarrow s\gamma$  branching ratio, relic density constraints and the possible new muon magnetic moment anomaly of the BNL E821 experiment, one can greatly sharpen predictions.

For the mSUGRA model, the  $m_h$  and  $b \rightarrow s\gamma$  bounds create a lower bound on  $m_{1/2}$  of  $m_{1/2} \gtrsim (300 - 400)\text{GeV}$  (i. e.  $m_{\tilde{\chi}_1^0} \gtrsim (120 - 140)\text{GeV}$ ). Thus puts the parameter space mostly in the  $\tilde{\tau}_1 - \tilde{\chi}_1^0$  co-annihilation domain, which strongly correlates  $m_0$  with  $m_{1/2}$ . For  $\mu > 0$  and  $m_{1/2} < 1\text{TeV}$ , one finds  $\sigma_{\tilde{\chi}_1^0-p} \lesssim 10^{-10}$  pb which is within the upper reach of future planned dark matter detectors, while for  $\mu < 0$  there will be large regions inaccessible to such detectors. If the  $a_\mu$  anomaly is confirmed, then  $\mu > 0$  and  $m_{1/2} < 800$  GeV.

Non-universal soft breaking models allow one to raise  $\sigma_{\tilde{\chi}_1^0-p}$  by a factor as large as 10 - 100, which could account for the large cross sections of the DAMA data. They can

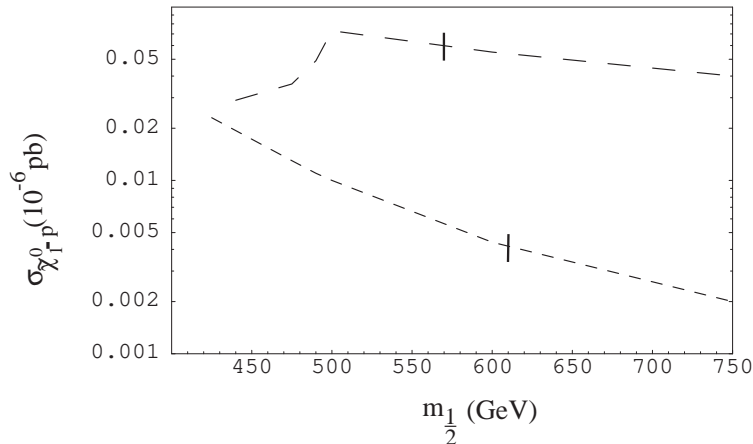


Figure 9:  $\sigma_{\tilde{\chi}_1^0-p}$  as a function of  $m_{1/2}$  for  $\tan\beta = 40$ ,  $\mu > 0$ ,  $A_0 = m_{1/2}$  and  $m_h > 114$  GeV. The lower curve is for the bottom of the  $\tilde{\tau}_1 - \tilde{\chi}_1^0$  co-annihilation corridor, and the upper curve is for the top of the  $Z$  channel band. The termination at low  $m_{1/2}$  is due to the  $b \rightarrow s\gamma$  constraint, and the vertical lines are the upper bound on  $m_{1/2}$  due to the lower bound of  $a_\mu$  of Eq. (5)[21].

also open new allowed regions of the  $m_0 - m_{1/2}$  plane from the  $Z$  channel annihilation in the relic density calculation. The new  $Z$ -channel regions have larger cross sections, though still below the DAMA region, but they should be accessible when CDMS is in the SOUDAN mine and to the GENIUS-TF detector. Thus dark matter detectors should be able to investigate the nature of SUSY soft breaking, i.e. the nature of the post-GUT physics that determine the soft breaking pattern.

## ACKNOWLEDGEMENTS

This work was supported in part by National Science Foundation Grant PHY-0070964 and PHY-0101015.

## References

- [1] G.L. Kane, L.-T. Wang, J.D. Wells, hep-ph/0108138.
- [2] E.A. Baltz, J. Edsjo, K. Freese, P. Gondolo, astro-ph/0109318.
- [3] V. Barger, F. Halzen, D. Hooper, C. Kao, hep-ph/0105182.
- [4] A. Bottino, N. Fornengo, S. Scopel, F. Donato, hep-ph/0105233.

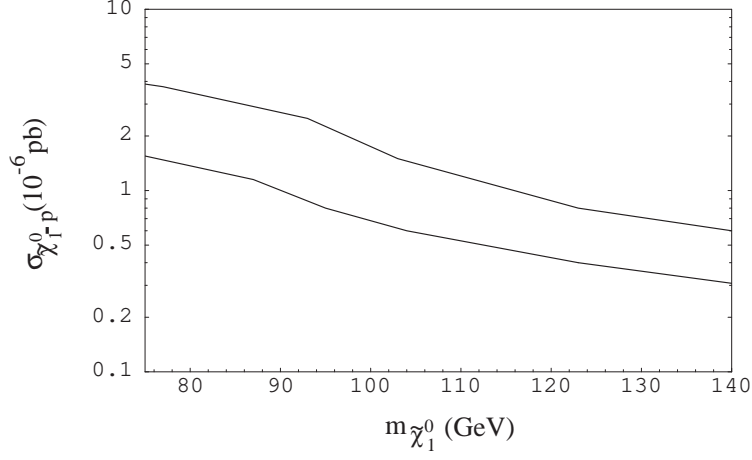


Figure 10: Maximum value of  $\sigma_{\tilde{\chi}_1^0-p}$  as a function of  $m_{\tilde{\chi}_1^0}$  for the nonuniversal model with  $\mu > 0$ ,  $\delta_1, \delta_3, \delta_4 < 0$ ,  $\delta_2 > 0$ . The lower curve is for  $\tan \beta = 7$ , the upper curve is for  $\tan \beta = 12$ .

- [5] A.H. Chamseddine, R. Arnowitt, P. Nath, Phys. Rev. Lett. **49** (1982) 970.
- [6] R. Barbieri, S. Ferrara, C.A. Savoy, Phys. Lett. B**119** (1982) 343; L. Hall, J. Lykken, S. Weinberg, Phys. Rev. D**27** (1983) (2359); P. Nath, R. Arnowitt, A.H. Chamseddine, Nucl. Phys. B**227** (1983) (121).
- [7] P. Igo-Kemenes, LEPC meeting, November 3, 2000 (<http://lephiggs.web.cern.ch/LEPHIGGS/talks/index.html>).
- [8] CLEO Collaboration, Phys. Rev. Lett. **87** (2001) 251807.
- [9] H.N. Brown et.al., Muon (g-2) Collaboration, Phys. Rev. Lett. **86** (2001) 2227.
- [10] M. Knecht, A. Nyffeler, hep-ph/0111058; M. Knecht, A. Nyffeler, E. De Raphael, hep-ph/0111059.
- [11] M. Hayakawa, T. Kinoshita, hep-ph/0112102; I. Blokland, A. Czernecki, K. Melnikov, hep-ph/0112117.
- [12] R.R. Akhmetshin et al., hep-ex/0112031.
- [13] R. Rattazi, U. Sarid, Phys. Rev. D**53** (1996) (1553).
- [14] M. Carena, M. Olechowski, S. Pokorski, C. Wagner Nucl. Phys. B**426** (1994) (269).
- [15] G. Degrandi, P. Gambino, G. Giudice, JHEP**0012** (2000) 009.
- [16] M. Carena, D. Garcia, U. Nierste, C. Wagner, Phys. Lett. B **499** (2001) 141.

- [17] R. Arnowitt, B. Dutta, Y. Santoso, Phys. Rev. D **64** (2001) 113010.
- [18] R. Arnowitt, B. Dutta, Y. Santoso, Nucl. Phys. B **606** (2001) 59.
- [19] J. Ellis, A. Ferstl, K. A. Olive, Phys. Lett. B **481** (2001) 304; Phys. Rev. D **63** (2001) 065016.
- [20] R. Arnowitt, P. Nath, Phys. Rev. D **56** (1997) 2820.
- [21] R. Arnowitt, B. Dutta, B. Hu, Y. Santoso, Phys. Lett. **B505**, (2001) 177.